

1 **Title:**

2 **Wide sampling of natural diversity identifies novel molecular signatures of C<sub>4</sub>**  
3 **photosynthesis**

4

5 **Authors:**

6 Steven Kelly<sup>1§\*</sup>, Sarah Covshoff<sup>2§</sup>, Samart Wanchana<sup>3\*§</sup>, Vivek Thakur<sup>3</sup>, W. Paul Quick<sup>3,4</sup>, Yu  
7 Wang<sup>5</sup>, Martha Ludwig<sup>6</sup>, Richard Bruskiewich<sup>3</sup>, Alisdair R. Fernie<sup>7</sup>, Rowan F. Sage<sup>8</sup>, Zhijian Tian<sup>9</sup>,  
8 Zixiang Yan<sup>9</sup>, Jun Wang<sup>9</sup>, Yong Zhang<sup>10</sup>, Xin-Guang Zhu<sup>11,12</sup>, Gane Ka-Shu Wong<sup>9,10,13,\*</sup>, Julian M.  
9 Hibberd<sup>2,\*</sup>

10

11 **Affiliations:**

12 <sup>1</sup>Department of Plant Sciences, South Parks Road, University of Oxford, Oxford, OX1 3RB, UK.

13 <sup>2</sup>Department of Plant Sciences, Downing Street, University of Cambridge, Cambridge, CB2 3EA,  
14 UK.

15 <sup>3</sup>C<sub>4</sub> Rice Center, International Rice Research Institute (IRRI), DAPO Box 7777, Metro Manila,  
16 Philippines.

17 <sup>4</sup>Department of Animal and Plant Sciences, University of Sheffield, Western Bank, Sheffield S10  
18 2TN, UK.

19 <sup>5</sup>Institute for Genomic Biology, University of Illinois at Urbana Champagne, IL USA, 61801.

20 <sup>6</sup>School of Chemistry & Biochemistry, The University of Western Australia, 35 Stirling Highway,  
21 Crawley, WA 6009, Australia.

22 <sup>7</sup>Max-Planck-Insitüt für Molekulare Pflanzenphysiologie, Am Mühlenberg 1, D-14476 Potsdam-  
23 Golm, Germany.

24 <sup>8</sup>Department of Ecology and Evolutionary Biology, University of Toronto, 25 Willcocks Street,  
25 Toronto, ON M5S 3B2, Canada.

26 <sup>9</sup>BGI-Shenzhen, Beishan Industrial Zone, Yantian District, Shenzhen 518083, China.

27 <sup>10</sup>Department of Biological Sciences, University of Alberta, Edmonton AB, T6G 2E9, Canada.

28 <sup>11</sup>CAS-MPG Partner Institute for Computational Biology, Chinese Academy of Sciences, Shanghai,  
29 China 200031.

30 <sup>12</sup>State Laboratory for Hybrid Rice Research, Changsha, Hunan, China.

31 <sup>13</sup>Department of Medicine, University of Alberta, Edmonton AB, T6G 2E1, Canada.

32

33 \*For correspondence: email - jmh65@cam.ac.uk, gane@ualberta.ca, steven.kelly@plants.ox.ac.uk

34

35 **Introductory paragraph**

36

37 **Much of biology is associated with convergent traits, and it is challenging to determine the**  
38 **extent to which underlying molecular mechanisms are shared across phylogeny. By**  
39 **analyzing plants representing eighteen independent origins of C<sub>4</sub> photosynthesis, we**  
40 **quantified the extent to which this convergent trait utilises identical molecular mechanisms.**

41 **We demonstrate that biochemical changes that characterise C<sub>4</sub> species are recovered by**  
42 **this process, and expand the paradigm by four metabolic pathways not previously**  
43 **associated with C<sub>4</sub> photosynthesis. Furthermore, we show that expression of many genes**  
44 **that distinguish C<sub>3</sub> and C<sub>4</sub> species respond to low CO<sub>2</sub>, providing molecular evidence that**  
45 **reduction in atmospheric CO<sub>2</sub> was a driver for C<sub>4</sub> evolution. Thus the origin and architecture**  
46 **of complex traits can be derived from transcriptome comparisons across natural diversity.**

47

48

49 **Main text:**

50 The evolution of complex traits has produced great diversity in form and function across the  
51 living world. A large number of similar complex traits have evolved independently in multiple  
52 disparate lineages indicating that common responses to environmental selection can result in  
53 convergent phenotypes<sup>1,2</sup>. The C<sub>4</sub> photosynthetic pathway, with at least 65 independent origins  
54 distributed across the angiosperms<sup>3</sup>, is considered one of the most remarkable examples of  
55 evolutionary convergence in eukaryotes. Thus the C<sub>4</sub> pathway represents an attractive trait with  
56 which to determine whether phylogenetically diverse species can be examined to discover the  
57 shared molecular basis of complex convergent phenotypes.

58 Using a comparative approach, we analyzed gene expression of 30 C<sub>4</sub> and 17 C<sub>3</sub> species  
59 representing 18 independent evolutionary origins of C<sub>4</sub> photosynthesis (Fig. 1A,B). This set of  
60 species includes representatives from all seven orders within the eudicotyledons known to have  
61 evolved C<sub>4</sub> photosynthesis (Fig. 1a, Supplemental File 1)<sup>4</sup>. This sampling expands upon previous  
62 transcriptome studies with C<sub>3</sub> and C<sub>4</sub> eudicot plants in *Cleomaceae*, *Asteraceae* and *Portulaceae*<sup>1–</sup>  
63 <sup>3</sup>. RNA was isolated from leaves of all species, sequenced and subjected to *de novo* transcriptome  
64 assembly. Collectively these samples comprise 850 million reads that were assembled into 1.5  
65 million contigs of which 1.1 million were assigned to orthogroups (Fig. 1B, Supplemental File 1)  
66 using a machine learning approach<sup>5</sup>. Analysis of the correlation in mRNA abundance estimates  
67 between species revealed that species did not cluster according to their photosynthetic type but  
68 rather according to phylogenetic relationship (Supplemental File 2). That is, C<sub>4</sub> species of *Flaveria*  
69 are more similar to C<sub>3</sub> *Flaveria* than to C<sub>4</sub> species from other genera, and thus variation in gene  
70 expression underlying phenotypic convergence is not the primary determinant of differences in  
71 mRNA abundance between C<sub>3</sub> and C<sub>4</sub> species.

72 Comparison of the transcriptomes from C<sub>3</sub> and C<sub>4</sub> species identified 149 genes that showed  
73 altered transcript abundance between C<sub>3</sub> and C<sub>4</sub> species in all 18 lineages: 113 that were more  
74 abundant and 36 less abundant in all C<sub>4</sub> species (Table 1, Supplemental File 3, Supplemental File  
75 4). This set includes many genes encoding components of C<sub>4</sub> photosynthesis that are known to  
76 change during evolution of the C<sub>4</sub> pathway (Fig. 2A, Supplemental File 5, and Supplemental File  
77 6). Four transcription factors were more abundant in all C<sub>4</sub> species (*PAT1*, *ZML2*, *SHR* and a

78 *bHLH* transcription factor of unknown function). Both *PAT1* and *ZML2* act to induce the expression  
79 of genes encoding photosynthesis proteins downstream of phytochrome and cryptochrome  
80 signalling respectively<sup>6,7</sup> while *SHR* is a validated regulator of C<sub>4</sub> Kranz anatomy in *Zea mays*<sup>8-10</sup>.  
81 Thus three of the four transcription factors have previously been identified as playing a role in the  
82 regulation of photosynthesis gene expression or leaf anatomy, both of which are altered during the  
83 evolution of C<sub>4</sub> photosynthesis. The uncharacterised bHLH domain transcription factor has no  
84 known functional role, but has previously been described as being upregulated in the bundle  
85 sheath (BS) cells of the C<sub>3</sub> plant *Arabidopsis thaliana*<sup>11</sup>. It is therefore possible that this bHLH  
86 transcription factor plays an ancestral role in the BS of C<sub>3</sub> species that has become enhanced in all  
87 C<sub>4</sub> lineages. Wide sampling of natural diversity therefore indicates that there is convergence in the  
88 recruitment of key regulators of gene expression in independent lineages of C<sub>4</sub> species.

89 Transcripts encoding 16 proteins comprising four metabolic pathways that have not previously  
90 been associated with C<sub>4</sub> photosynthesis were detected as differentially abundant between C<sub>4</sub> and  
91 C<sub>3</sub> species (Fig. 2B, Supplemental File 7). These pathways described below encompass: a novel  
92 carbon concentrating pathway involving the GABA shunt; metabolism associated with regeneration  
93 of phosphoenolpyruvate (PEP), the primary CO<sub>2</sub> acceptor in the C<sub>4</sub> pathway; modifications to  
94 pyruvate metabolism that prevent diversion of pyruvate from the C<sub>4</sub> cycle into non-photosynthetic  
95 pathways such as lipid and branched amino acid biosynthesis; and a photorespiratory pathway  
96 previously associated with chlorophyte algae (Supplemental File 7).

97 The abundance of transcripts encoding a key component of the  $\gamma$ -aminobutyric acid (GABA)  
98 shunt was increased in all C<sub>4</sub> compared with C<sub>3</sub> species. In the conventional model for NAD-ME  
99 type C<sub>4</sub> photosynthesis, aspartate synthesised in mesophyll (M) cells is shuttled to mitochondria in  
100 the BS where it is transaminated to oxaloacetate by aspartate amino transferase (ASP1), reduced  
101 to malate by NAD-dependent malate dehydrogenase (NAD-MDH), and then decarboxylated to  
102 pyruvate which can then return to the M (Fig. 2a). Although *ASP1* transcripts were more abundant  
103 in all C<sub>4</sub> species that we studied, this was not the case for the later steps in the NAD-ME pathway  
104 (Supplemental File 7). Instead, we propose that oxaloacetate is used to feed the tricarboxylic acid  
105 (TCA) cycle in BS cells. Here, 2-oxoglutarate synthesised by the TCA cycle can be converted to  
106 glutamate and decarboxylated by glutamate decarboxylase (GAD4) to GABA, resulting in release

107 of CO<sub>2</sub> and return of carbon skeletons as succinate to the TCA cycle (Fig. 2, Supplemental File 5,  
108 Supplemental File 7). This proposed pathway provides both a novel mechanism to transfer CO<sub>2</sub> to  
109 the BS using CO<sub>2</sub> that was fixed by phosphoenolpyruvate carboxylase (PEPC) in the M, and a  
110 source of ATP in the BS by using NADH generated by the running the TCA cycle for oxidative  
111 phosphorylation (Fig. 2B, Supplemental File 5, Supplemental File 6). Two orthogonal approaches  
112 provide evidence that this cycle functions to concentrate CO<sub>2</sub> in the C<sub>4</sub> BS. First, computational  
113 modelling revealed that the additional ATP this pathway provides to BS cells resulted in an  
114 increased CO<sub>2</sub> assimilation rate irrespective of C<sub>4</sub> subtype under low light conditions  
115 (Supplemental File 8). Moreover, when PEPCK is used for decarboxylation this increase in CO<sub>2</sub>  
116 assimilation rate was maintained under high light (Supplemental File 8). Second, biochemical  
117 evidence for this pathway has in fact been reported previously - after <sup>14</sup>C labelled glutamate was  
118 fed to isolated BS strands in *Zea mays*<sup>12</sup>, radiolabel is rapidly released and redistributed to other  
119 metabolites in a manner that is most parsimoniously explained by glutamate decarboxylase  
120 mediated decarboxylation followed by re-fixation of labelled CO<sup>2</sup> by RuBisCO. Thus, sampling the  
121 natural diversity of C4 species uncovered an adjunct CO<sub>2</sub> concentrating pathway that is supported  
122 by biochemical data and a metabolic model of C<sub>4</sub> photosynthesis.

123 To maintain flux through the C<sub>4</sub> pathway, PEP supply is critical as it is the entry point of the  
124 cycle. Transcripts encoding a chloroplastic phosphoglucomutase (PGM) and an enolase (ENO)  
125 were more abundant in all C<sub>4</sub> compared with C<sub>3</sub> species (Fig. 2B, Supplemental File 7). These  
126 proteins facilitate conversion of Calvin-Benson cycle intermediates to PEP (Fig. 2B), providing an  
127 additional route for transfer of photo-assimilated carbon to the M, and consequently regeneration  
128 of the initial carbon acceptor. Transcripts encoding pyruvate kinase (PK), which catalyzes the  
129 reverse reaction, were less abundant in C<sub>4</sub> compared with C<sub>3</sub> species (Fig. 2B). A reduction in the  
130 amount of the cognate protein would limit futile cycling between PEP and pyruvate during C<sub>4</sub>  
131 photosynthesis. The third pathway detected in our analysis indicates pyruvate metabolism has  
132 been modified to prevent diversion of pyruvate from C<sub>4</sub> photosynthesis into non-photosynthetic  
133 pathways such as lipid and branched amino acid biosynthesis. Transcripts encoding pyruvate  
134 dehydrogenase kinase (PDK) were more abundant (Fig. 2B), and aceto-lactate synthase (ALS)  
135 less abundant, in all C<sub>4</sub> compared with C<sub>3</sub> leaves (Supplemental File 7). As PDK deactivates

136 pyruvate dehydrogenase by phosphorylation and ALS channels pyruvate into the synthesis of  
137 branched-chain amino acids, these alterations would support the core C<sub>4</sub> cycle by reducing loss of  
138 pyruvate from photosynthetic pools.

139 The fourth pathway that we propose is modified in all C<sub>4</sub> compared with C<sub>3</sub> species has been  
140 previously associated with algae rather than land plants. Chloroplasts of chlorophyte algae enclose  
141 their RuBisCO in structures called pyrenoids. These structures facilitate an increased CO<sub>2</sub>  
142 concentration around RuBisCO resulting in reduced photorespiration<sup>13</sup>. These algae also lack the  
143 peroxisome-based photorespiratory pathway that evolved in the common ancestor of  
144 embryophytes and charophyte algae<sup>14</sup>. Although the ancestral chlorophyte photorespiratory  
145 pathway involving glycolate dehydrogenase (GlcDH) and an alanine:glyoxylate amino transferase  
146 (ALAAT2) is still active in C<sub>3</sub> plants, flux of glycolate through this pathway is low compared with the  
147 peroxisome-based pathway<sup>15</sup>. Our analysis indicates that in all 18 C<sub>4</sub> lineages there is a concerted  
148 increase in abundance of transcripts encoding key components of the chlorophyte algal pathway,  
149 specifically GlcDH and ALAAT2 (Fig. 2B, Supplemental File 7). Two scenarios may explain this  
150 change during C<sub>4</sub> evolution. First, the chlorophyte photorespiratory pathway plays a role in C<sub>4</sub>  
151 photosynthesis. Second, GlcDH plays a role in converting some dihydroxyacetone phosphate  
152 (DHAP) produced in the Calvin-Benson cycle of BS cells to pyruvate *via* the methylglyoxal pathway  
153 enabling the use of some DHAP to maintain the C<sub>4</sub> cycle (Supplemental File 9). In this latter  
154 scenario, ALAAT2 would still process photorespiratory glyoxylate that had been produced in the  
155 peroxisome by glycolate oxidase. Both proposed scenarios require a source of NAD<sup>+</sup> and in this  
156 context it is noteworthy that both transcripts encoding Complex I of the respiratory electron transfer  
157 chain and the plant uncoupling mitochondrial protein 1 (PUMP1) were upregulated in C<sub>4</sub> species  
158 (Fig. 2B). Together, these would increase regeneration of NAD<sup>+</sup> and de-couple some proton flux  
159 through Complex I from ATP synthesis. Moreover, this increase in NAD<sup>+</sup> would also support  
160 photorespiratory glycine decarboxylase and utilise NADH from the TCA cycle (Fig. 2B).

161 We also evaluated whether transcriptome sampling across a deep phylogeny could be used to  
162 clarify selective forces promoting C<sub>4</sub> evolution. Low atmospheric CO<sub>2</sub> has been proposed to be a  
163 key driver of C<sub>4</sub> evolution<sup>16</sup>, and analysis of *A. thaliana* identified genes responsive to low CO<sub>2</sub> in  
164 plants<sup>17</sup>. Thirty-one of the 113 genes that were more abundant in all C<sub>4</sub> species sampled showed

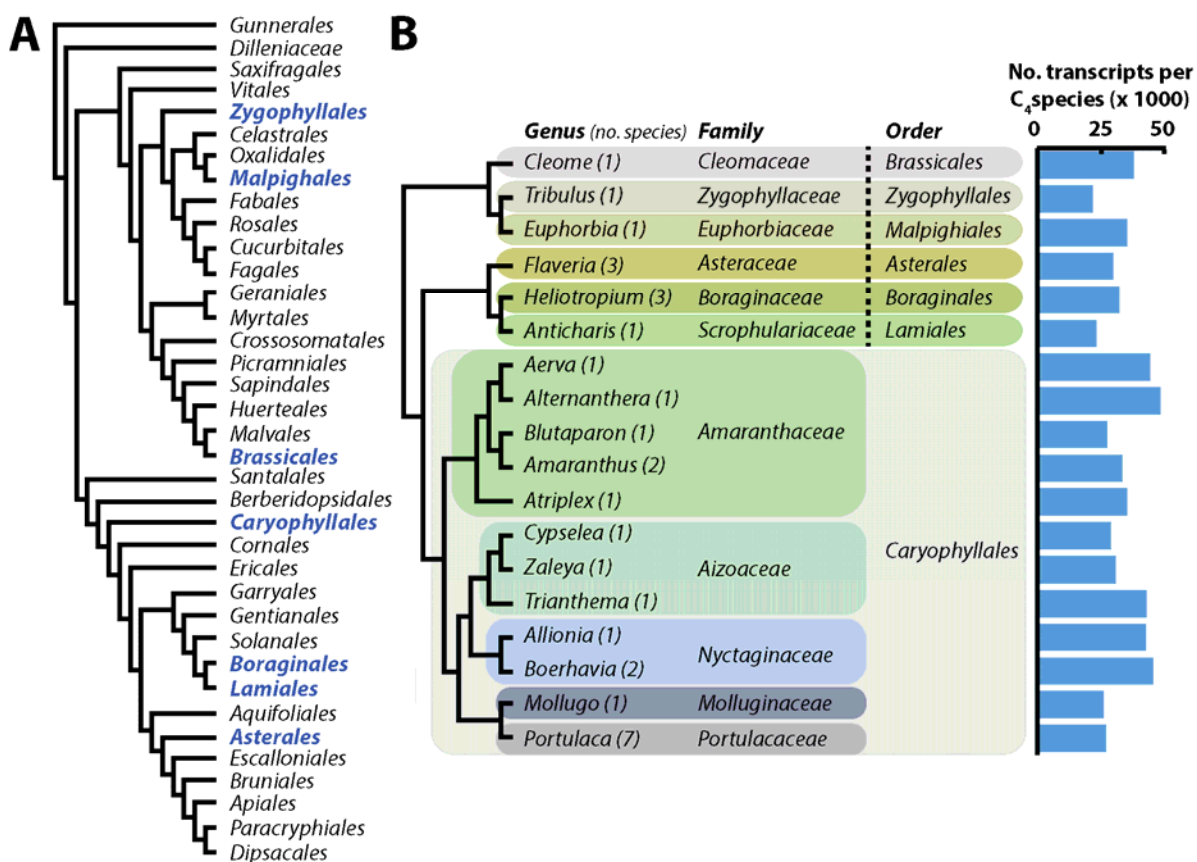
165 increased expression in *A. thaliana* grown under low CO<sub>2</sub> (Fig. 3, Supplemental File 10). As the  
166 probability of such an overlap is low ( $p = 4 \times 10^{-9}$ ), these data indicate that there is a significant  
167 association between genes that are expressed highly in C<sub>4</sub> species and those that are more  
168 abundant in C<sub>3</sub> *A. thaliana* grown under low CO<sub>2</sub>. There is also a significant association between  
169 genes that are more abundant under low CO<sub>2</sub> and those that are less abundant in all C<sub>4</sub> plants ( $p =$   
170  $1 \times 10^{-5}$ , Fig. 3). However, nine of these twelve genes encode components of the photorespiratory  
171 pathway and the remaining three are unknown proteins predicted to localize to the chloroplast and  
172 are thus implicated in photorespiratory processes (Supplemental File 11). These results are  
173 consistent with the hypothesis that low atmospheric CO<sub>2</sub> concentration induced changes in gene  
174 expression that facilitated C<sub>4</sub> evolution. The molecular mechanisms that underpin this response  
175 remain to be identified. In the future it will be informative to investigate the extent to which other  
176 ecological drivers such as heat, drought and salinity alter gene expression and potentially target  
177 genes that are then recruited into this complex trait. In addition, the data also reveal that a set of  
178 genes that are more abundant in C<sub>4</sub> species are preferentially expressed in the BS cells of C<sub>3</sub>  
179 species and thus indicate that neofunctionalisation of BS cells utilized pathways already present in  
180 this cell type (Supplemental File 5, Supplemental File 12). Thus these data also provide molecular  
181 support for the hypothesis that expansion and specialization of the C<sub>3</sub> BS is an early and key step  
182 in the evolution of the C<sub>4</sub> phenotype<sup>19,18</sup>.

183 Finally, the data identify four metabolic pathways previously unknown to be important for C<sub>4</sub>  
184 function, and identify a role for the GABA shunt pathway in concentrating CO<sub>2</sub> and generating ATP  
185 in the BS of all C<sub>4</sub> species. The re-emergence in plants of the peroxisome-based photorespiratory  
186 pathway from algae is to our knowledge, the first documented example of an evolutionary  
187 reversion being a key component of the advent of complexity and convergence in eukaryotic  
188 biology. We envisage that this approach of comparative transcriptome sampling of non-model  
189 species will now be used to provide insight into molecular signatures associated with complex  
190 traits across the tree of life. The fact that we recapitulated previous knowledge of C<sub>4</sub>  
191 photosynthesis, but also significantly extended the functional model of C<sub>4</sub> metabolism, implies  
192 there is much more to be discovered about this pathway.

193



195 **Figures**

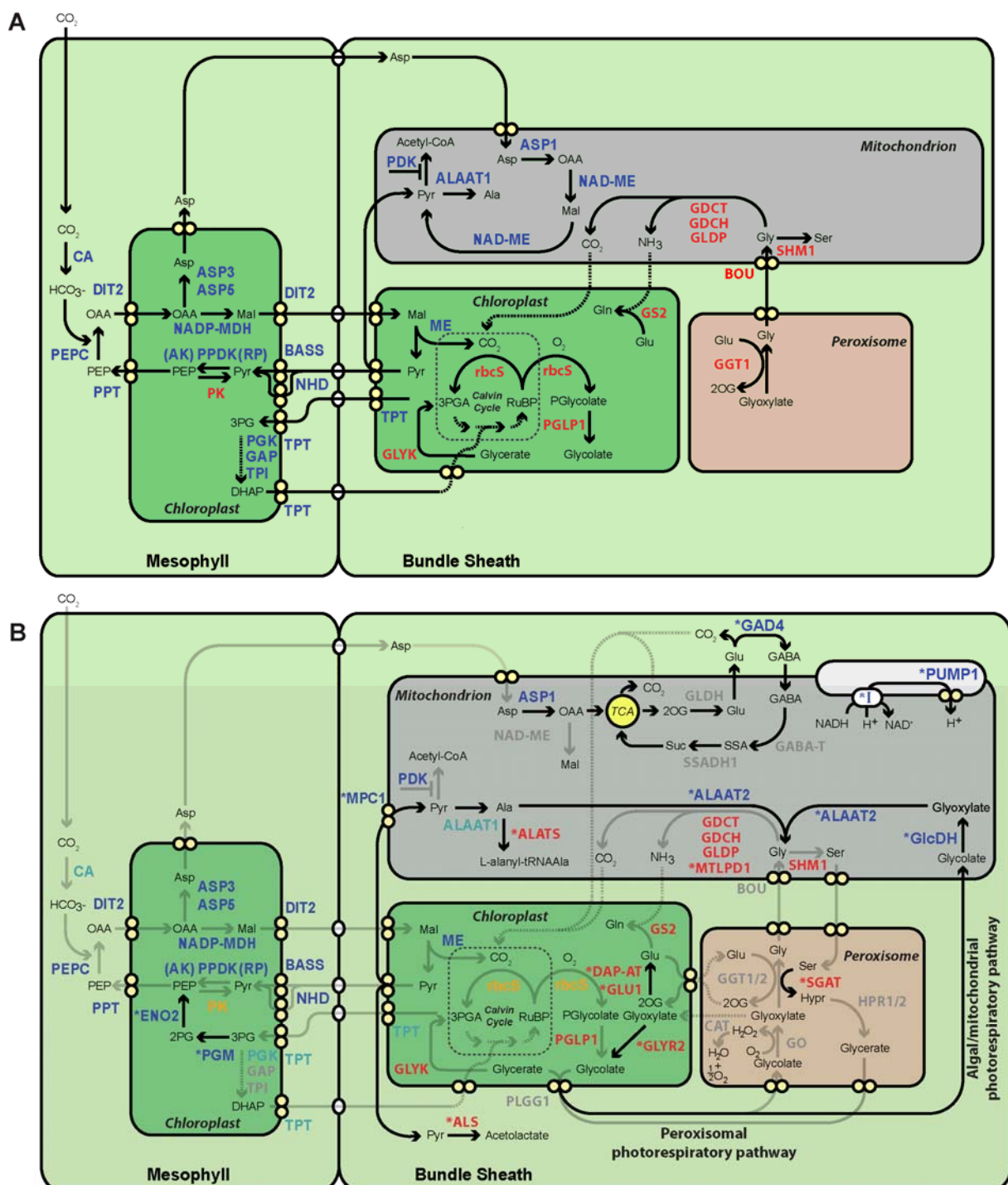


196

197 **Fig. 1:** Within the eudicotyledons C<sub>4</sub> photosynthesis has evolved in eleven families from 7 different  
198 orders. (A) Phylogenetic tree showing the seven orders containing C<sub>4</sub> species (blue). (B)  
199 Phylogenetic tree showing the relationship between the eighteen genera (eleven families)  
200 encompassing thirty C<sub>4</sub> species sampled in this study. Numbers after the genus name indicate the  
201 number of C<sub>4</sub> species sampled. The mean number of *de novo* transcripts per species is indicated  
202 for each genus.

203

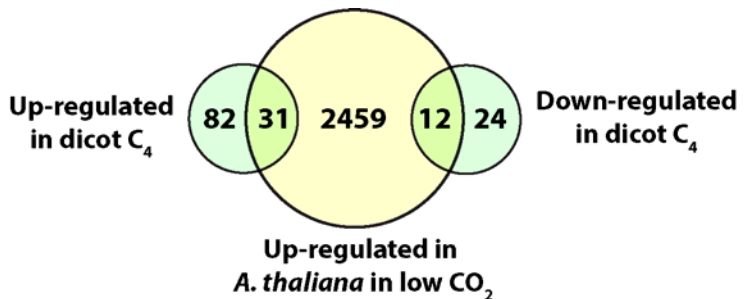
204



205  
206 this study. (A) Enzymes and transporters previously known to be upregulated (blue) and down-  
207 regulated (red) in C<sub>4</sub> compared with C<sub>3</sub> leaves are depicted according subcellular location and  
208 whether they are preferentially expressed in either mesophyll or bundle sheath cells. (B) After  
209 sequencing 30 C<sub>4</sub> and 17 C<sub>3</sub> species spanning the seven eudicotyledon orders known to have  
210 evolved C<sub>4</sub> photosynthesis an additional 16 genes consistently up (blue) or down regulated (red) in

212 C<sub>4</sub> compared with C<sub>3</sub> leaves were identified. Light blue and orange indicate transcripts for genes  
213 that are significantly upregulated and downregulated in all C<sub>4</sub> species when compared to all C<sub>3</sub>, but  
214 they fail to achieve significance with computational occlusion and resampling. For abbreviations of  
215 gene names see Supplemental File 10. TCA, tricarboxylic cycle.

216



217

218 **Fig. 3:** Overlap between genes that are upregulated in response to low CO<sub>2</sub> in *Arabidopsis*  
219 *thaliana* and that are up or downregulated in C<sub>4</sub> species.

220

Category	Cell	Chloroplast	Mitochondrion
Metabolic components	15 (8)	29 (10)	6 (4)
Signalling components	18 (2)	7 (1)	0 (0)
Transporters	4 (1)	9 (1)	2 (0)
Transcription regulators	4 (1)	0 (2)	0 (0)
Post transcription regulators	3 (1)	0 (0)	0 (0)
Other	3 (0)	2 (2)	0 (0)
Unknown	9 (3)	1 (0)	1 (0)

221 n= 113, n = 36 No. up-regulated (No. down-regulated)

222 **Table 1:** Summary of functional categories of genes differentially expressed between C<sub>4</sub> and C<sub>3</sub>  
223 leaves.

224 **References**

- 225 1 Stern, D. L. The genetic causes of convergent evolution. *Nature reviews. Genetics*  
226 **14**, 751-764, doi:10.1038/nrg3483 (2013).
- 227 2 Morris, S. C. Evolution: like any other science it is predictable. *Philosophical*  
228 *transactions of the Royal Society of London. Series B, Biological sciences* **365**, 133-  
229 145, doi:10.1098/rstb.2009.0154 (2010).
- 230 3 Sage, R. F. A portrait of the C4 photosynthetic family on the 50th anniversary of its  
231 discovery: species number, evolutionary lineages, and Hall of Fame. *Journal of*  
232 *experimental botany* **67**, 4039-4056, doi:10.1093/jxb/erw156 (2016).
- 233 4 Sage, R. F., Christin, P. A. & Edwards, E. J. The C(4) plant lineages of planet Earth.  
234 *Journal of experimental botany* **62**, 3155-3169, doi:10.1093/jxb/err048 (2011).
- 235 5 Aubry, S., Kelly, S., Kumpers, B. M., Smith-Unna, R. D. & Hibberd, J. M. Deep  
236 evolutionary comparison of gene expression identifies parallel recruitment of trans-  
237 factors in two independent origins of C4 photosynthesis. *PLoS genetics* **10**,  
238 e1004365, doi:10.1371/journal.pgen.1004365 (2014).
- 239 6 Torres-Galea, P., Hirtreiter, B. & Bolle, C. Two GRAS proteins, SCARECROW-  
240 LIKE21 and PHYTOCHROME A SIGNAL TRANSDUCTION1, function  
241 cooperatively in phytochrome A signal transduction. *Plant physiology* **161**, 291-304,  
242 doi:10.1104/pp.112.206607 (2013).
- 243 7 Shaikhali, J. *et al.* The CRYPTOCHROME1-dependent response to excess light is  
244 mediated through the transcriptional activators ZINC FINGER PROTEIN  
245 EXPRESSED IN INFLORESCENCE MERISTEM LIKE1 and ZML2 in *Arabidopsis*.  
246 *The Plant cell* **24**, 3009-3025, doi:10.1105/tpc.112.100099 (2012).
- 247 8 Wang, P., Kelly, S., Fouracre, J. P. & Langdale, J. A. Genome-wide transcript  
248 analysis of early maize leaf development reveals gene cohorts associated with the  
249 differentiation of C4 Kranz anatomy. *The Plant journal : for cell and molecular*  
250 *biology* **75**, 656-670, doi:10.1111/tpj.12229 (2013).
- 251 9 Slewinski, T. L. Using evolution as a guide to engineer kranz-type c4  
252 photosynthesis. *Frontiers in plant science* **4**, 212, doi:10.3389/fpls.2013.00212  
253 (2013).
- 254 10 Slewinski, T. L. *et al.* Short-root1 plays a role in the development of vascular tissue  
255 and kranz anatomy in maize leaves. *Molecular plant* **7**, 1388-1392,  
256 doi:10.1093/mp/ssu036 (2014).
- 257 11 Aubry, S., Smith-Unna, R. D., Boursnell, C. M., Kopriva, S. & Hibberd, J. M.  
258 Transcript residency on ribosomes reveals a key role for the *Arabidopsis thaliana*  
259 bundle sheath in sulfur and glucosinolate metabolism. *The Plant journal : for cell*  
260 *and molecular biology* **78**, 659-673, doi:10.1111/tpj.12502 (2014).
- 261 12 Weissmann, S. *et al.* Interactions of C4 Subtype Metabolic Activities and Transport  
262 in Maize Are Revealed through the Characterization of DCT2 Mutants. *The Plant*  
263 *cell* **28**, 466-484, doi:10.1105/tpc.15.00497 (2016).
- 264 13 Giordano, M., Beardall, J. & Raven, J. A. CO<sub>2</sub> concentrating mechanisms in algae:  
265 mechanisms, environmental modulation, and evolution. *Annual review of plant*  
266 *biology* **56**, 99-131, doi:10.1146/annurev.arplant.56.032604.144052 (2005).
- 267 14 Finet, C., Timme, R. E., Delwiche, C. F. & Marletaz, F. Multigene phylogeny of the  
268 green lineage reveals the origin and diversification of land plants. *Current biology :*  
269 *CB* **20**, 2217-2222, doi:10.1016/j.cub.2010.11.035 (2010).
- 270 15 Niessen, M. *et al.* Mitochondrial glycolate oxidation contributes to photorespiration  
271 in higher plants. *Journal of experimental botany* **58**, 2709-2715,  
272 doi:10.1093/jxb/erm131 (2007).

- 273 16 Ehleringer, J. R., Sage, R. F., Flanagan, L. B. & Pearcy, R. W. Climate change and  
274 the evolution of C<sub>4</sub> photosynthesis. *Trends in ecology & evolution* **6**, 95-99,  
275 doi:10.1016/0169-5347(91)90183-X (1991).
- 276 17 Li, Y., Xu, J., Haq, N. U., Zhang, H. & Zhu, X. G. Was low CO<sub>2</sub> a driving force of C<sub>4</sub>  
277 evolution: *Arabidopsis* responses to long-term low CO<sub>2</sub> stress. *Journal of*  
278 *experimental botany* **65**, 3657-3667, doi:10.1093/jxb/eru193 (2014).
- 279 18 Williams, B. P., Johnston, I. G., Covshoff, S. & Hibberd, J. M. Phenotypic landscape  
280 inference reveals multiple evolutionary paths to C<sub>4</sub> photosynthesis. *eLife* **2**, e00961,  
281 doi:10.7554/eLife.00961 (2013).
- 282 19 Christin, P. A. *et al.* Anatomical enablers and the evolution of C<sub>4</sub> photosynthesis in  
283 grasses. *Proceedings of the National Academy of Sciences of the United States of*  
284 *America* **110**, 1381-1386, doi:10.1073/pnas.1216777110 (2013).
- 285
- 286

287 **Acknowledgements:**

288 This work was funded by a Bill and Melinda Gates Foundation and a Department for International  
289 Development award to IRRI and sub-awards to SK, XZ, RFS and JMH. The 1000 Plants (1KP)  
290 initiative, led by GKS, is funded by the Alberta Ministry of Advanced Education, Alberta  
291 Innovates Technology Futures (AITF), Innovates Centre of Research Excellence (iCORE), Musea  
292 Ventures, BGI-Shenzhen and China National Genebank (CNGB), and DSERC Discovery grants to  
293 RFS. SK is a Royal Society University Research Fellow. This work was supported by the European  
294 Union's Horizon 2020 research and innovation programme under grant agreement no 637765.

295

296 **List of Supplementary Materials:**

297 **Supplemental File 1:** Summary of C<sub>3</sub> and C<sub>4</sub> species sampled in this study. Each species is  
298 classified by its photosynthetic pathway, its family and order. The number of sequenced reads,  
299 assembled contigs, annotated contigs, and assembly N50 for each species obtained are also  
300 listed.

301

302 **Supplemental File 2:** Phylogenetic position accounts for more variance in mRNA abundance than  
303 photosynthetic pathway. The heat map depicts the Spearman's ranked correlation coefficient ( $\rho$ )  
304 between each species pair computed from global mRNA abundance estimates. The hierarchical  
305 cluster (tree to the left of the heat map) was computed directly from the correlation coefficients by  
306 converting these correlation coefficients to distance estimates. The distance estimate between two  
307 species A and B is evaluated as  $1 - \rho$ . i.e.  $d(A,B) = 1 - \rho$ . A tree is then inferred from these

308 distance estimates using the minimum evolution principle. Names of C<sub>4</sub> species are shown in blue.

309

310 **Supplemental File 3:** Summary of genes showing differential expression between C<sub>4</sub> and C<sub>3</sub>  
311 leaves. The likelihood of differential expression is provided considering all species. Also provided  
312 is the proportion of resampling tests in which the gene was detected as consistently differentially  
313 regulated between C<sub>3</sub> and C<sub>4</sub> species. The mean and standard deviation of the expression  
314 estimate is provided for the C<sub>3</sub> and C<sub>4</sub> cohort as well as the number of samples that were identified  
315 as outliers and masked prior to differential expression testing. The expected count for each gene  
316 for each species is also provided.

317

318 **Supplemental File 4:** The subset of genes from Supplemental File 3 that received 100% support  
319 from computational occlusion and resampling.

320

321 **Supplemental File 5:** Additional information.

322

323 **Supplemental File 6:** Genes previously reported to be differentially expressed in C<sub>4</sub> compared  
324 with C<sub>3</sub> leaves.

325

326 **Supplemental File 8:** Four additional metabolic pathways identified in this study. In each case the  
327 relative expression is given for C<sub>3</sub> (grey bars) and C<sub>4</sub> (green bars) species. \* indicates a likelihood  
328 of differential expression  $\geq 0.95$  and 100% support from computational occlusion and resampling.  
329 n.s. indicates a non-significant difference between the C<sub>3</sub> and C<sub>4</sub> expression levels. (A) GABA  
330 shunt. (B) Phosphoenolpyruvate regeneration. (C) First step of branched chain amino acid  
331 biosynthesis. (D) Chlorophyte photorespiratory pathway.

332

333 **Supplemental File 8:** Modelling the addition of the GABA shunt to the C4 photosynthesis.

334

335 **Supplemental File 9:** Schematic illustrating an alternative hypothesis for the function of the  
336 glycolate dehydrogenase gene that is potentially a lactate dehydrogenase. This pathway would

337 convert dihydroxyacetone phosphate to pyruvate *via* methylglyoxal.

338

339 **Supplemental File 10:** Genes that were up-regulated in all C<sub>4</sub> species and also up-regulated in  
340 response to low atmospheric CO<sub>2</sub> in the C<sub>3</sub> plant *Arabidopsis thaliana*.

341

342 **Supplemental File 11:** Genes that were down-regulated in all C<sub>4</sub> species and also up-regulated in  
343 response to low atmospheric CO<sub>2</sub> in the C<sub>3</sub> plant *Arabidopsis thaliana*.

344

345 **Supplemental file 12:** The overlap between the genes differentially regulated in all C<sub>4</sub> species with  
346 other datasets. A) Comparison of transcripts upregulated in all C<sub>4</sub> species with those preferentially  
347 expressed in *Arabidopsis thaliana* bundle sheath cells. B) Comparison of genes identified as  
348 differentially abundant in all C<sub>4</sub> species compared to those identified as differentially abundant  
349 between C<sub>3</sub> and C<sub>4</sub> species of *Flaveria*. C) Analysis of the cell type specific expression in *Zea*  
350 *mays* and *Setaria italica* of the orthologues of the genes identified as up-regulated in all C<sub>4</sub> species  
351 in this study.

352

353 **Supplemental File 13:** Genes that were up-regulated in all C<sub>4</sub> species and also up-regulated in in  
354 bundle sheath cells of the C<sub>3</sub> plant *Arabidopsis thaliana*.

355

356 **Supplemental File 14:** Full names and accession numbers for all genes shown in Fig. 2.

357

358 **Supplementary Methods:** Detailed descriptions of the data sources and methods.

359

360

361 **Author contributions**

362 SK, GKS, RB, RFS, SC and JMH conceived the work. SC and RFS acquired the plant collection  
363 and mRNA, while SK, VT, SW, WPQ, XGZ, YW, GKS, ML, RB, JW, YZ, ZY, ZT, ARF and RFS  
364 conducted the analysis. SK designed and developed the bioinformatic analyses. SK and JMH  
365 interpreted the data and wrote the paper.